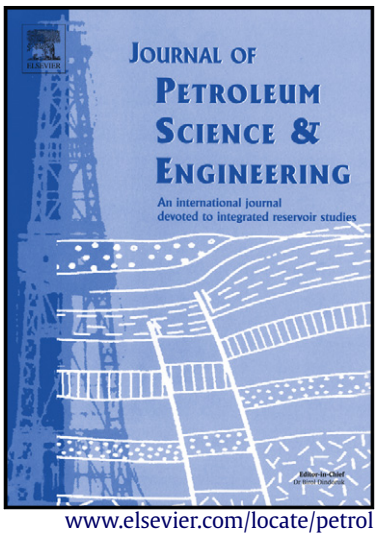

www.elsevier.com/locate/petrol

An automated simple algorithm for realistic pore network extraction from micro-tomography Images

Arash Rabbani, Saeid Jamshidi, Saeed Salehi

PII: S0920-4105(14)00269-1
DOI: http://dx.doi.org/10.1016/j.petrol.2014.08.020
Reference: PETROL2774

To appear in: *Journal of Petroleum Science and Engineering*

Received date: 24 December 2013
Accepted date: 12 August 2014

Cite this article as: Arash Rabbani, Saeid Jamshidi, Saeed Salehi, An automated simple algorithm for realistic pore network extraction from micro-tomography Images, *Journal of Petroleum Science and Engineering,* http://dx.doi.org/10.1016/j.petrol.2014.08.020

An Automated Simple Algorithm for Realistic Pore Network Extraction from Micro-Tomography Images

Arash Rabbani[1], Saeid Jamshidi[2], Saeed Salehi[3,*]

[1] Petroleum University of Technology, Tehran, Iran.

[2] Chemical and Petroleum Engineering Department, Sharif University of Technology, Tehran, Iran.

[3] College of Engineering, University of Louisiana at Lafayette, USA

Abstract

Using 3-D scanned data to analyze and extract pore network plays a vital role in investigation of porous media's chrateristics. In this paper, a new simple method is developed to detect pores and throats for analyzing the connectivity and permeability of the network. This automated method utilizes some of the common and well-known image processing functions which are widely accessible by researchers and this has led to an easy algorithm implementation. In this method, after polishing and quality control of images, using City-block Distance Function and Watershed Segmentation Algorithm, pores and throats are detected and 3-D network is produced. This method can also be applied on 2-D images to extract some characteristics of the porous media such as pore and throat size distribution. The results of network extraction were verified by comparing the distribution of coordination number with a prevalent method in the literature.

Keywords: Micro-Tomography Images, City-block Distance Function, Watershed Segmentation Algorithm, Pore Network Extraction.

1. Introduction

Pore network modeling is one of the primary means to simulate hydraulic behavior of porous media in micro scale level. Network models that represent the void space of a rock by a lattice of pores connected by throats can predict relative permeability once the pore geometry and wettability are known (Dong & Blunt, 2009). The predictive value of network models depends on the accuracy of imaging and the correspondence of network via real porous rocks (Sheppard et al., 2005). There are three different ways in which a 3-D representation of the void space of a rock can be obtained (Al-Kharusi & Blunt, 2007); a) description of the sedimentary process by which the rock is formed, b) two point or multiple point statistics to reconstruct 3-D images using 2-D image data, c) micro-CT scanning tools to create a 3D image. The development of computational methods to analyze the 3-D structure of pore networks has advanced significantly with the advent of Synchrotron CMT (Computed Micro Tomography) generating 3-D data sets at the micron scale level (Youssef et al., 2007). In order to interpret and simplify the 3-D volume data sets, the main challenge is to determine which every void space is exactly pore or throat. Although, the continuous and integrated void volume of porous media is hardly dividable to distinct pores and throats, it is inevitable to make some simplifying assumptions. There are two common approaches in the literature which aim to extract simplex pore network from real 3-D

* Corresponding author: Email: sxs9435@louisiana.edu

volume data: a) Maximal Inscribed Spheres and pore space distance approach (Jones et al., 2006), b) Skeletonizing and thinning methods (Al-Raoush & Willson, 2005). A concise literature review about the precedent methods of pore network extraction is provided in Table 1.

Table 1. Some of previous Pore Network Extraction methods and brief description

Method	Description	Developers
Simple Statistical	Simple Statistical Method using phase binarization describes how size and shape of pores affects the flow.	(Rezanezhad et al., 2009)
Inscribed Circles	Draws circles inscribed by pore walls and centered by the farthest points from grains to extract pores and throats.	(Sweeney & Martin, 2003)
Master-Slave Spheres	Defines two types inscribes spheres, Masters and Slaves, which is the bigger and smaller balls respectively compared to their neighbors.	(Silin & Patzek, 2006)
Maximal Ball Clustering	Divides inscribed balls to subsections attending the severity of being Master or Slave and denotes the local minima of sphere size as throats and vice versa as pores.	(Dong & Blunt, 2009)
Medial Axis Transform	Quantitative method characterizes void structure via Burn Number distribution analysis	(Lindquist et al., 1996)
Skeletonization	Obtains detailed geometric and topological description of pore network using the skeleton of the pore space as a basis to estimate the effective hydraulic and electrical conductance of individual flow paths identified with skeleton links.	(Liang, Ioannidis, & Chatzis, 2000)
Inscribed ball via Skeleton	Based on the three-dimensional Skeletonization that simplifies the pore space to networks in the form of nodes connected to paths coupled with Dilation algorithms developed to generate inscribed spheres on the nodes and paths of the medial axis to represent pore-bodies and pore-throats of the network, respectively.	(Al-Raoush & Willson, 2005)
Extremal distance map	Based on the extremal structures of the distance map of the pore space defines a merge concept that accomplishes a hierarchical merge using the significance of the pore separations.	(Homberg et al., 2012)
Velocity Based	Is based on 3D thinning of the velocity field in the pore space. The velocity field is calculated from a solution of the Stokes equations directly on the rock microstructure image.	(Dong et al., 2008)
Grain Recognition Based	Grains are identified by partitioning the solid phase. By knowing the grains, pore space can then be divided into polyhedra using Voronoi tessellation and the edges of the Voronoi polyhedra define the pore skeleton.	(Øren & Bakke, 2003)
Watershed Based	Applying anisotropic diffusion filter to remove noise while preserving significant features. Perform un-sharp mask sharpening filter which enhances edges and using combination of watershed and active contour methods for segmentation of the grey-scale data.	(Sheppard et al., 2004)

With all these methods, pre-processing and/or post-processing is required to remove excess pores and throats. For instance, in Skeletonization methods this usually means pruning the skeleton, whereas for maximal ball methods it usually involves merging adjacent regions (Wildenschild & Sheppard, 2013). Dong et al. (2008) presents a comparative study on four different network extraction methods available in the literature. They have found the Medial Axis method produce networks which contain more isolated and single connected pores than the Maximal Ball and Velocity Based networks. Dong et al. (2008) stated that for the sample with highest level of

noise, the applied Medial Axis algorithm failed to identify a realistic pore network and pore sizes determined by the Velocity Based and Maximal Ball networks tend to be similar. In addition, the pore sizes for the Medial Axis and Grain Recognition networks are relatively similar, but slightly larger than those of the Velocity based and Maximal Ball networks. Although, Maximal Ball method provides reliable results, it was observed that this approach is relatively CPU intensive among other methods in which requires modifications (Byholm et al., 2006).

This paper presents a new computational algorithm to extract pore network characteristics automatically which can present the realistic structure of pores and throats. In this method, by coupling two well-known image processing algorithms known as distance function and watershed segmentation, pores and throats are directly detected and separated. Coordination number or connectivity of pore network is easily obtained by analyzing the abutting pores and throats and counting the number of throats connected to each pore. Pore connectivity is one of the most important parameters determining the hydraulic characteristics of the porous medium. Not-interconnected porous martial have no permeability and vice versa.

Distance function calculates the distance between each pixel in the void volume of the porous media and the close by occupied pixel by the solids. In order to digitize pore volumes, binary images are utilized and every segment of porous media is converted to a binarized map which contains 1 for grains or solids and 0 for pores or voids (Maurer et al., 2003). Distance function appears in four different forms of generating contour lines or planes; a) Euclidean, b) City-block, c) Chessboard, d) Quasi-Euclidean (Rosenfeld & Pfaltz, 1966).

In the watershed segmentation, it is stated that intuitively, a drop of water falling on a topographic relief flows towards the "nearest" minimum. The "nearest" minimum is that minimum which lies at the end of the path of steepest descent. In terms of topography, this occurs if the point lies in the catchment basin of that minimum. The watershed line is the basic tool for segmenting images in mathematical morphology (Malpica et al., 1997). A rigorous definition is given in terms of a distance function called topographic distance. If the topographical function is itself a distance function, then the topographical distance becomes identical with the geodesic distance function and the watershed becomes identical with the skeleton by zone of influence (Meyer, 1994). Watershed has been used previously to analyze the sand beds segmentation and granular size (Sime & Ferguson, 2003).

2. Methodology

Although Watershed algorithm is powerful tool for segmentation, its application for rock network extraction does not straightforwardly lead to the acceptable results. In the present study, a practical and general workflow has been presented using well-known image processing functions in order to makes it possible for researcher to rerun this method using different software applications.

The first step in segmenting the porous media and network extraction is to use the proposed algorithm on 2-D images of sedimentary rocks. The aim is to breakdown the monolithic void structure of rock into specific pores and throats connecting to each other. Initially, two connected bodies should be detached by these image processing algorithms.

The watershed transform is a key building block for morphological segmentation (Dougherty & Lotufo, 2003). A classical approach for producing edge images is to apply a gradient and then threshold the resulting gradient image to produce a binary edge image. The most important difficulty with this approach is how to select an appropriate threshold value (Dougherty &

Lotufo, 2003). Watershed provides a fast and efficient method for segmentation and separation of attached clusters of objects (Malpica et al., 1997).

In order to understand this algorithm better, consider two connected binary objects as in shown in Figure 1. Assume that the white area of objects has depth. The depth of each pixel increases by increment of the distance of the pixel from the nearest black pixel. It means that in the center of each grain indicates the local deepest point in Figure 2. These two holes are called *Catchment basins*. Now, consider that water comes up in these basins because of rainfall (flooding). The first contact line that the water in two basins encounters by coming up is known as *watershed ridge line.* After this level, the water in two basins is connected. The line is interpreted as throat and two round objects are considered as pores. By cutting the structure on watershed ridge line, two pores will be detected and separated as well as the connecting throat.

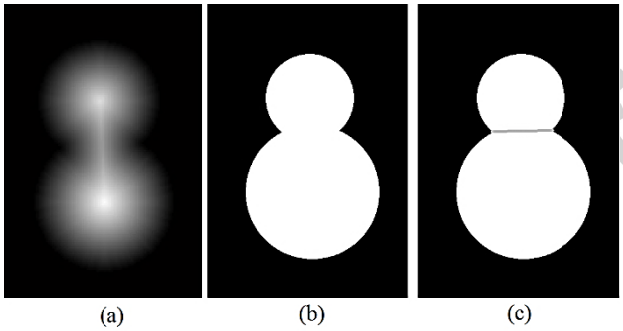

Figure 1. Sample for watershed method, (a) is the grayscale distance map, (b) the original binary image and (c) segmented pores

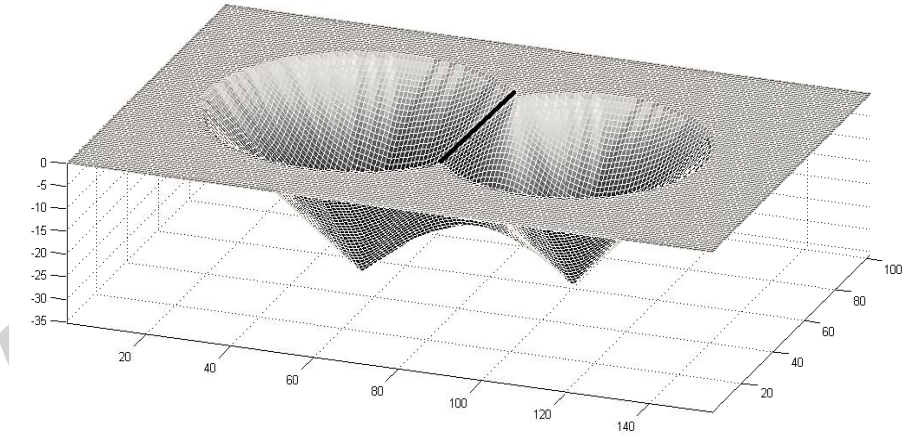

Figure 2. Watershed approach clarification, Catchment basins and watershed ridge line

Preparation of distance plays an important role in detection and distinction of connected pores. In this regards, for each pixel inside the object with coordination of x_i and y_i, the distance from nearest black pixel should be calculated. In Figure 1 (a), brighter area represents farther point from black region. Consider the black points with coordination of x_b and y_b. In order to find

distance map, the distance between one specific white pixel and an arbitrary black pixel should be minimized. This Euclidean distance is:

$$D_b = \sqrt{(x_b - x_i)^2 + (y_b - y_i)^2} \qquad (1)$$

Where D_b is distance between a specific white pixel (x_i , y_i) and an arbitrary black pixel (x_b , y_b). This function is known as the Euclidean form. For Manhattan or City-block distance map the formula for calculating distance is expressed in equation 2.

$$D_b = |x_b - x_i| + |y_b - y_i| \qquad (2)$$

Watershed segmentation is sensitive to image noises. In noised images, many fake watershed ridge lines may be detected. In order to prevent this error, median filter for alleviating the noise intensity in distance map is suggested. Here, the neighborhood pixel interval used for filtering is 5 by 5 pixels. As it is visible in Figure 3, in the lack of median filtering over distance map many parallel fake ridge lines will be detected (Figure 3 (b)) while there is more adequate boundary detection for image that received filtering. Majority morphological transform is also a common image processing function which keeps the main parts of structure and removes the minor roughness or noises which may distract the Watershed function from being accurate (Figure 4). Majority transform interval is 5 pixel in this study and needs to be done before preparing distance map while median filtering is required after distance mapping.

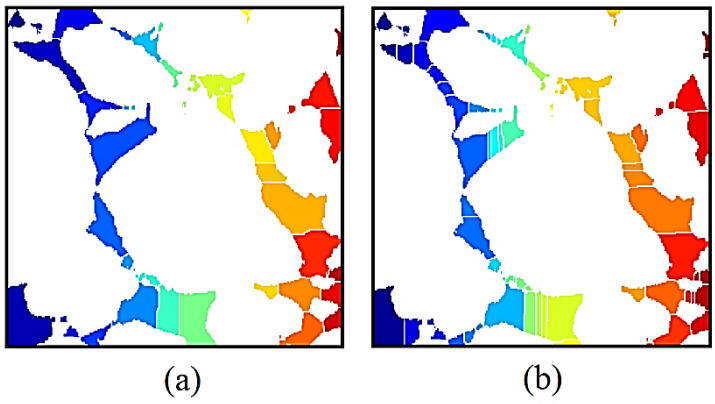

Figure 3. Comparison between a 2D sandstone sample with median filtering of distance function (a) and the same image with no filtering (b)

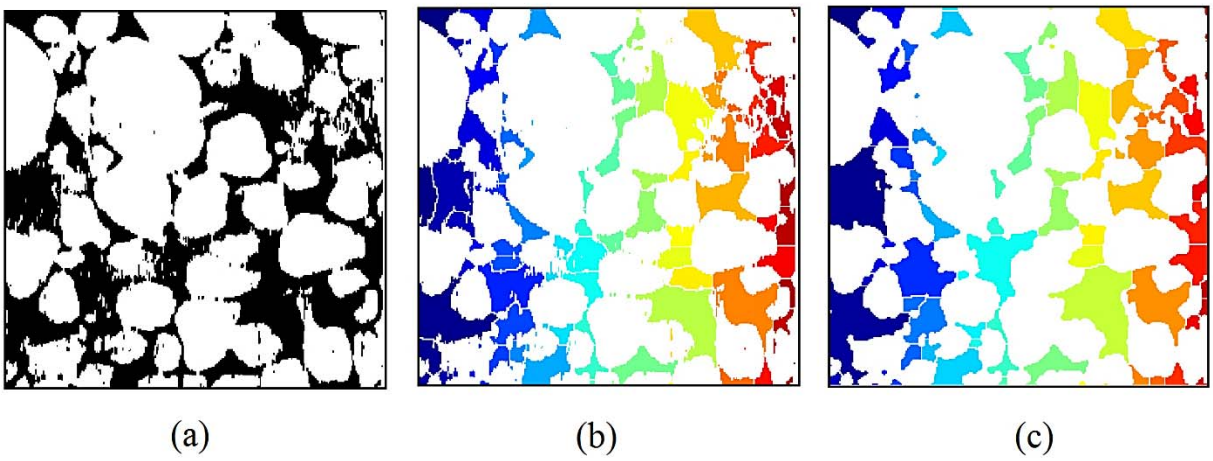

Figure 4. Effect of Majority morphological transform on more clear and distinct pore/throat detection, original image (a), Watershed segmentation with Median filtering but without performing Majority transform (b) and Watershed segmentation with Median filtering and Majority transform

As mentioned, there are four different forms of distance function (Figure 5). In this study, it is found that the best form of distance function for distinction between rock pores and throats is City-block. Contour lines in this function has shown sharp change in the boundary between the two pores. Further investigation and test show that Chessboard form is also appropriate but not the best for this purpose. Both City-block and Chessboard forms create angular and cubical contours which intersect with curved pore walls in explicit boundaries while watershed flooding and this leads to better and clearer pore-throat distinction. Those breakpoints visible in the curvature of contours in City-block and Chessboard image, represents the *watershed ridge line* which can be obtained by connecting produced points together.

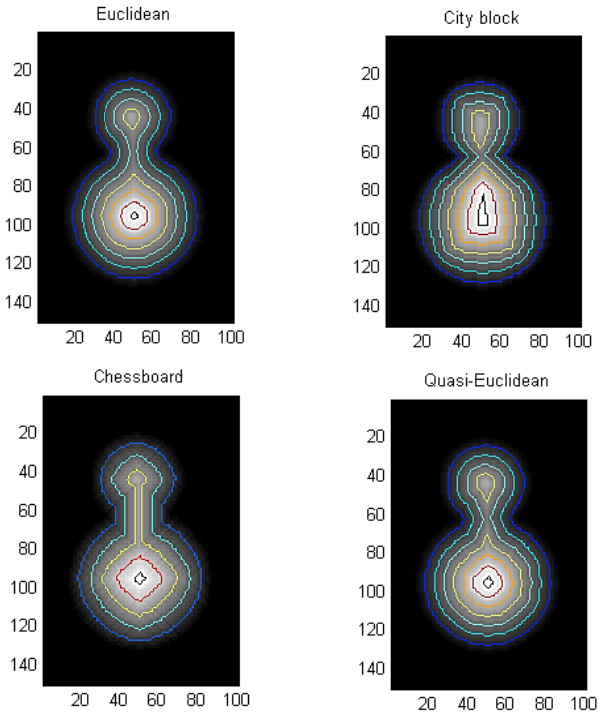

Figure 5. Four different forms of distance function for 2D pore structures

The same procedure should be applied for 3-D image analysis by extending distance transform and watershed to three dimensions. In 3-D, watershed ridge line will change to a tiny curved cortex. Figure 6 illustrates comparison for four different distance functions. According to the explicit change in the shape of City-block and Chessboard distance contours at throat area, those methods seem to be more suitable for separation of pores while smooth curves between two pores lead to count them as a single pore. While extending to 3-D, the median filter noise removal process should be implemented to prohibit fake throat detection. Common and commercial watershed algorithms usually put zero for watershed ridge lines in their output. Consequently, it would be very convenient to find throats of porous structure using commercial and educational image processing packages such as MATLAB or OPENCV. In the present work, a code has been written using MATLAB to perform the image processing algorithms via its toolbox. If the 3D array of ridge points is subtracted from the initial 3-D array of volume data, a binary array of separated pores will be obtained.

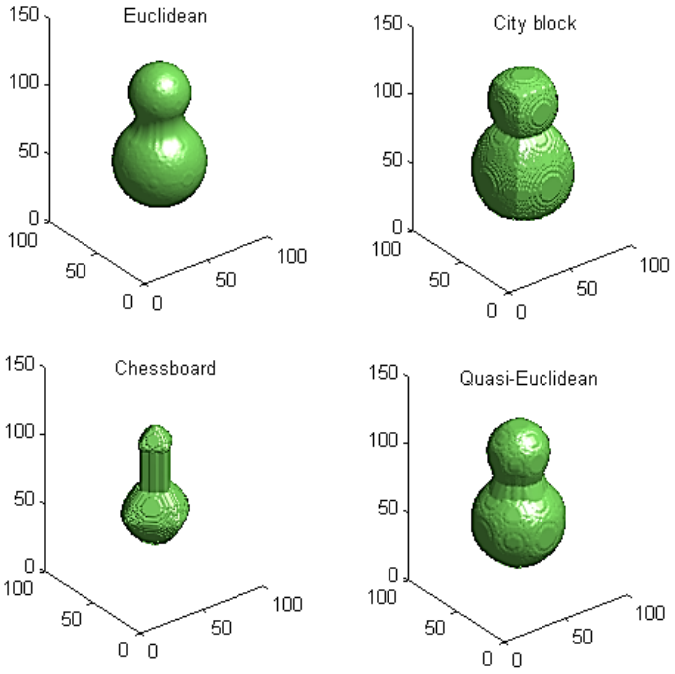

Figure 6. Four different forms of distance function for 3D implementation on sample pore structures

The pixels connectivity is of great importance when using distance function and watershed algorithm. For example, results may change depending on whether flooding pixels are diagonal or cubical. The pixel connectivity chosen in this work is 26 for 3-D and 8 for 2-D image analysis which is a comprehensive approach. To summarize, the workflow of the proposed algorithm is delineated as steps in Figure 7.

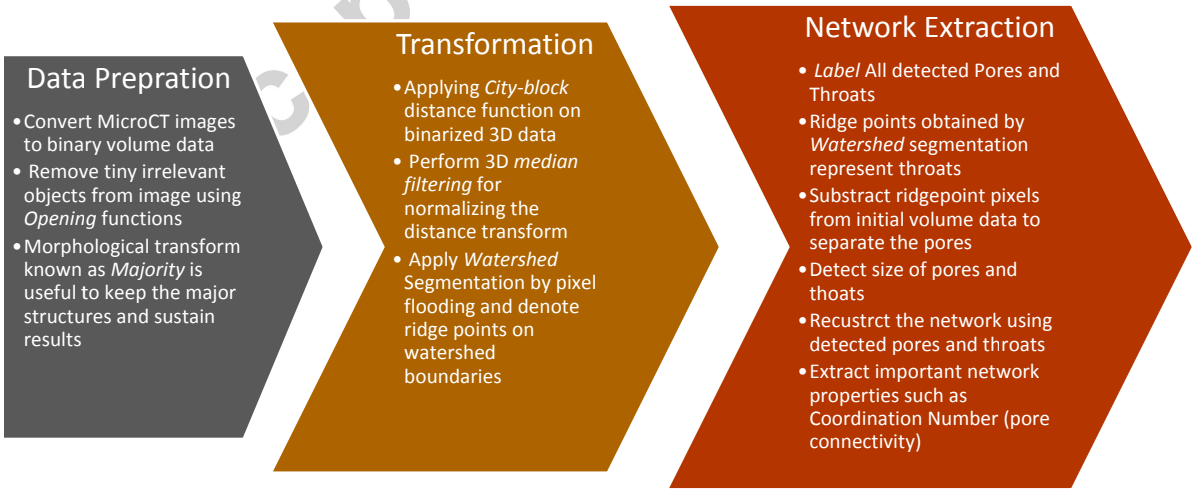

Figure 7. Workflow of the proposed algorithm to detect and extract pore network of porous medium

Considering the complicated internal structure of rocks it is not possible to model the network without applying simplifying assumptions. In the presented method, it has been assumed that the radius of model pores are equal to the radius of realistic pores with the same volume. Consequently the porosity of network model remain as the same as rock porosity. Also, throats has been modeled as cylinders which connecting the pores alongside the direction between the center of pores. In addition, cylindrical throats of model have volume equal to the real throats volume by stipulating an appropriate radius.

3. Results and Discussions

The developed algorithm for porous media segmentation is implemented on two various rock types where the 3-D volume data and analysis were available in the literature. Berea Sandstone and a heterogenic Carbonate sample are studied and after segmentation, their pore network is extracted. The analysis of coordination number of samples is in the agreement with previous reputable method known as Maximal Ball (Dong & Blunt, 2009) (Figure 17 and Figure 18). Table 2 compares the average coordination number of networks between Watershed and Maximal ball method.

Table 2. Comparison between average coordination numbers obtained by two methods

Rock	Maximal Ball Method average coordination number	Watershed Method average coordination number
Berea Sandstone	3.91	3.57
Carbonate Sample	3	2.7

Figure 8 and Figure 9 illustrate the 3D volume data of samples studied in this work. As it is visible, Berea is homogenous whereas Carbonate sample is not. Although the major changes in image resolution may transform the generated networks, the variety in the pore structures of different rocks and fabrics did not affect the results.

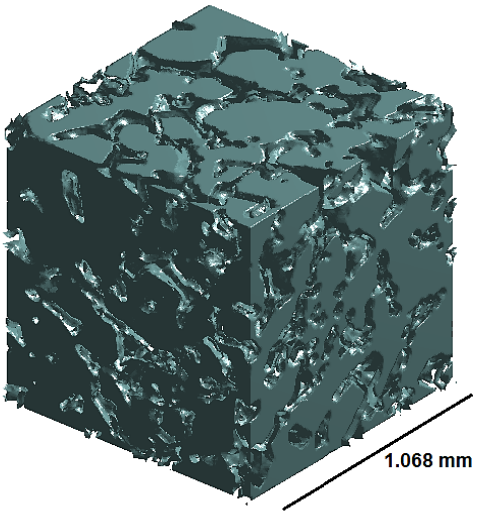

Figure 8. 3D volume data of Berea sample, Resolution of Micro CT: 5.3 microns per pixel

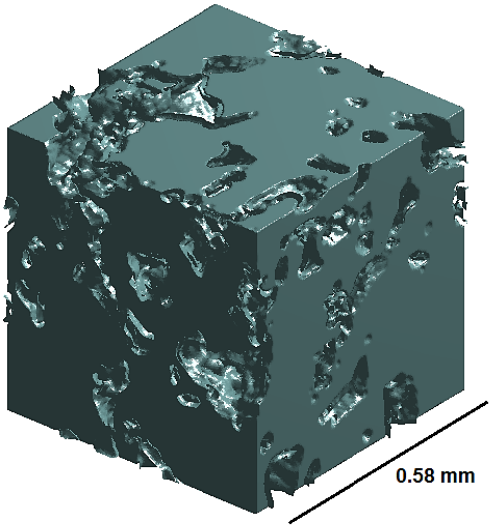

Figure 9. 3D volume data of carbonate sample, Resolution of Micro CT: 2.9 micron per pixel

Furthermore, this methodology can be applied in two dimensional analysis such as thin sections of rock and other porous media. In addition to detect pore connectivity, this can be also applied for detecting individual pore throat's size and orientation. The connectivity of pores in 2-D is almost proportional to 3-D pore connectivity known as Coordination number. Figure 10 and Figure 11 present two random cross sections of rock samples which are used to perform watershed segmentation and pore-throat detection. Using this analysis the pore size distribution and throat size distribution of rocks are accessible using simple 2-D imaging. Pore detection results are illustrated in the Figure 12 and Figure 13. Different colors were used to distinguish each detected pore. Initial images indicate that the explicit distinction between pores and throats is not possible even by hand especially in the carbonate sample which contains severe

heterogeneity. The omitted white lines are throats which are already detected in the watershed algorithm.

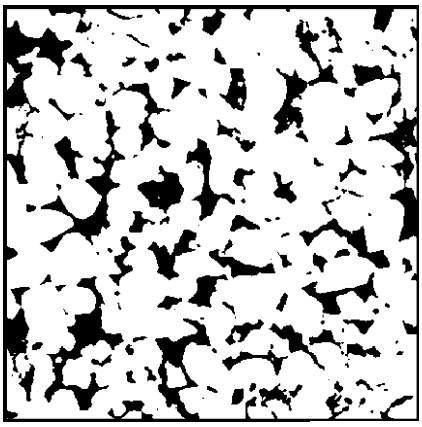

Figure 10. Random Cross section of Berea Sample used for 2D analysis

Figure 11. Random cross section of Carbonate Sample used for 2D analysis

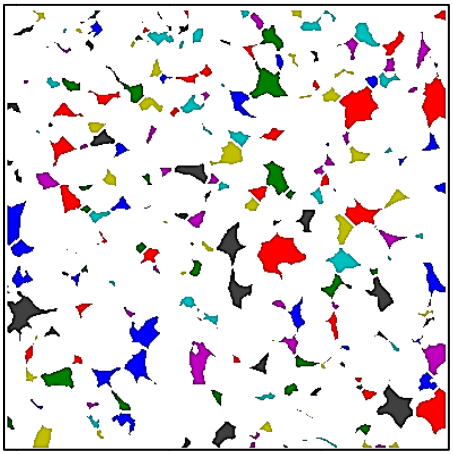

Figure 12. Segmented 2D sample of Berea in which pores and throats are detected and each pore appears in a different color

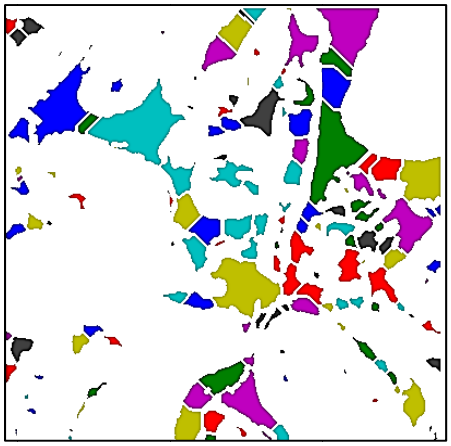

Figure 13. Segmented 2D sample of Carbonate in which pores and throats are detected and each pore appears in a different color

In 3-D, the procedure is more complicated and time consuming. As throats appear in 2-D analysis as lines, in 3-D images they are shown as curved tiny cortexes. Figure 14 represents the realistic geometry of network throats detected by Watershed segmentation algorithm for Berea Sandstone sample. In 3-D segmentation, throats are pixels in which the growing nuclei of center of pores (catchment basins) meet each other at first. In another word, consider nuclei at the center of pores that enlarge gradually corresponded to the distance map 3-D contours. At each pace, nuclei advance to the next distance level until two nuclei from two different pores touch the surface of each other. By continuing the nuclei enlargement, intersected pixels of two nuclei forms a cortex which represents the throat between those pores. Connectivity of throats to pores is investigated by labelling and testing them by putting labelled throat between detected pores. After determination of coordination number of each pore, by finding the size and position of each pore and throat, the simplified pore network is accessible. Figure 15 and Figure 16 show the results on Sandstone and Carbonate samples studied in this work. The radius of pores and also throats are shown in the half of its real size to make the interior structure more visible.

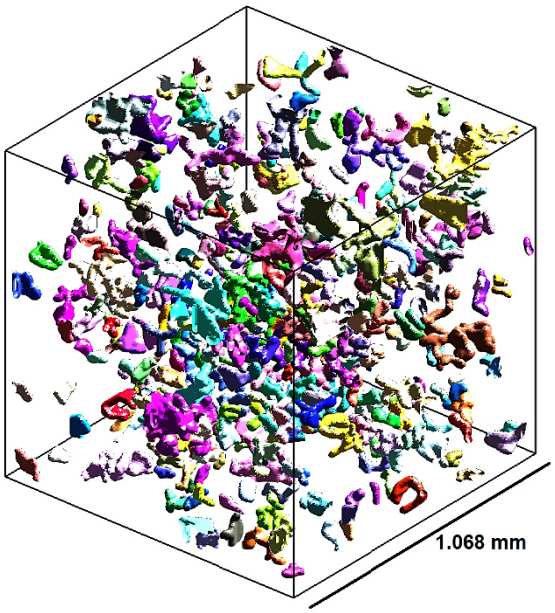

Figure 14. Real shape of throats in the Berea Sandstone network detected by Watershed algorithm

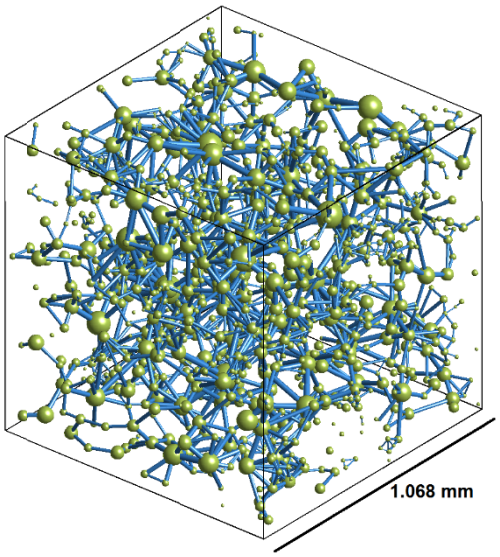

Figure 15. Extracted network of Berea sample with reduced (half) radius of pores and throats for better delineation

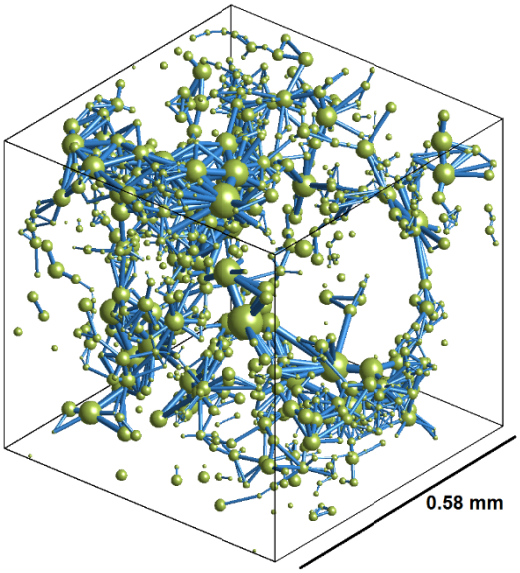

Figure 16. Extracted network of Carbonate sample with reduced (half) radius of pores and throats for better delineation

Determination of coordination number for samples using this method represents results which are corresponds to the previous common method; the maximal ball. The results of maximal ball analysis are obtained from Dong and Blunt (2009) and comparison has been presented in Figure 17 and Figure 18. Although Carbonate sample contains severe heterogeneity as it is depicted visually in Figure 16, the presented method successfully estimates the distribution of pore network connectivity. Average absolute error in the estimated relative frequency chart is 0.007 for Berea sample and 0.02 for carbonate sample. Considering the fact that the results of Maximal ball method itself as reference may suffer uncertainty, error values are not numerically reliable.

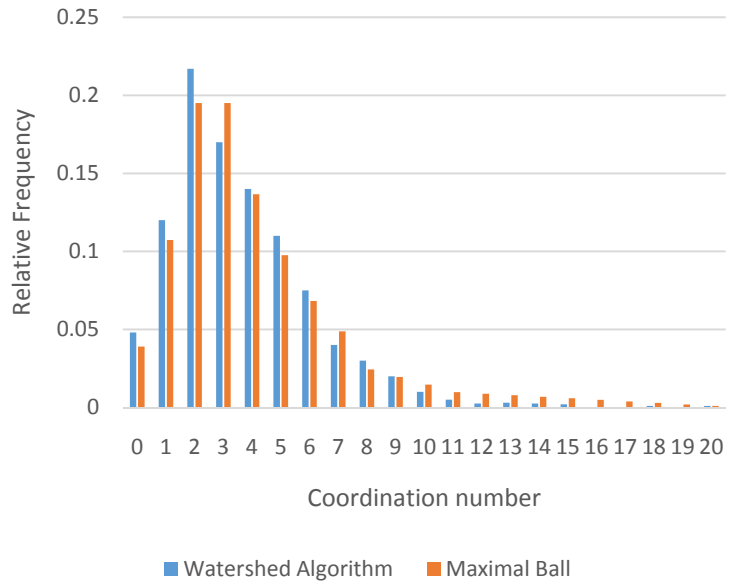

Figure 17. Coordination number distribution for Berea sample obtained by the proposed method (Watershed) and a common method (Maximal Ball)

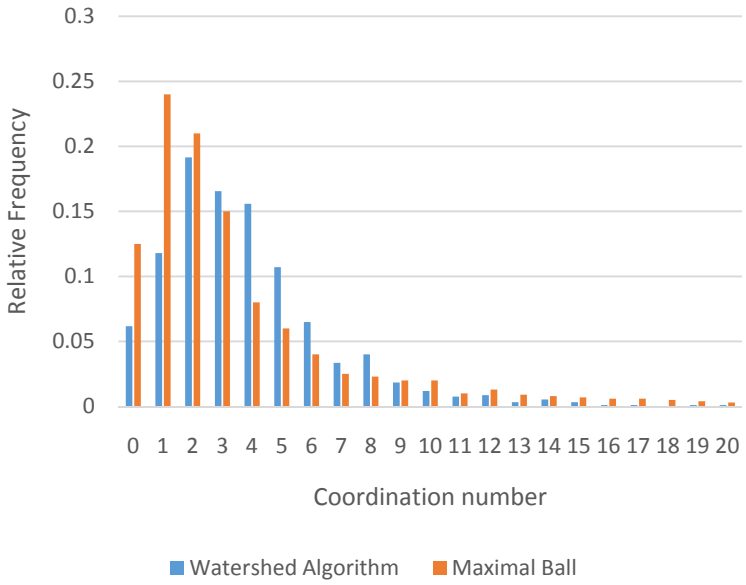

Figure 18. Coordination number distribution for Carbonate sample obtained by the proposed method (Watershed) and a common method (Maximal Ball)

4. Conclusion

In the present study, a new algorithm for extraction of pore network from 3-D Realistic Micro-tomography images has been developed. In this automated method, after pre-filtration and quality control using Majority and Opening functions, images are transformed by City-block distance function and are exposed to median filtering for noise removal. Performing segmentation using watershed algorithm leads to detect throats and consequently to differentiate pores. By assuming pores as spheres and throats as cylinders, a clarified pore network model is

generated. The Coordination number calculated from this approach is in agreement with the results of maximal inscribed ball which is one of the most common method for this purpose. Here, a practical and general workflow has been developed using well-known image processing functions which makes it possible for researcher to rerun this method using different commercial or open source image processing software packages or libraries.

5. References

Al-Kharusi, A. S., & Blunt, M. J. (2007). Network extraction from sandstone and carbonate pore space images. *Journal of petroleum science and engineering, 56*(4), 219-231.

Al-Raoush, R., & Willson, C. (2005). Extraction of physically realistic pore network properties from three-dimensional synchrotron X-ray microtomography images of unconsolidated porous media systems. *Journal of Hydrology, 300*(1), 44-64.

Byholm, T., Toivakka, M., & Westerholm, J. . (2006). The application of morphological algorithms on 3-dimensional porous structures for identifying pores and gathering statistical data. *WSEAS Transactions on Information Science and Applications, 3(12)*, 2374-2380.

Dong, H., & Blunt, M. J. (2009). Pore-network extraction from micro-computerized-tomography images. *Physical review E, 80*(3), 036307.

Dong, H., Fjeldstad, S., Alberts, L., Roth, S., Bakke, S., Øren, P. E., & Numerical Rocks, A. S. (2008). Pore network modelling on carbonate: a comparative study of different micro-CT network extraction methods. *International Symposium of the Society of Core Analysts, Abu Dhabi*.

Dougherty, E. R., & Lotufo, R. A. (2003). *Hands-on morphological image processing*.

Homberg, U., Baum, D., Prohaska, S., Kalbe, U., & Witt, K. J. (2012). *Automatic Extraction and Analysis of Realistic Pore Structures from μCT Data for Pore Space Characterization of Graded Soil*. Paper presented at the ICSE6 Paris.

Jones, M. W., Baerentzen, J. A., & Sramek, M. (2006). 3D distance fields: A survey of techniques and applications. *Visualization and Computer Graphics, IEEE Transactions on, 12*(4), 581-599.

Liang, Z., Ioannidis, M., & Chatzis, I. (2000). Permeability and electrical conductivity of porous media from 3D stochastic replicas of the microstructure. *Chemical engineering science, 55*(22), 5247-5262.

Lindquist, W. B., Lee, S. M., Coker, D. A., Jones, K. W., & Spanne, P. (1996). Medial axis analysis of void structure in three-dimensional tomographic images of porous media. *Journal of Geophysical Research: Solid Earth (1978–2012), 101*(B4), 8297-8310.

Malpica, N., Ortiz de Solorzano, C., Vaquero, J. J., Santos, A., Vallcorba, I., Garcia-Sagredo, J. M., & Pozo, F. d. (1997). Applying watershed algorithms to the segmentation of clustered nuclei.

Maurer Jr, C. R., Qi, R., & Raghavan, V. (2003). A linear time algorithm for computing exact Euclidean distance transforms of binary images in arbitrary dimensions. *Pattern Analysis and Machine Intelligence, IEEE Transactions on, 25*(2), 265-270.

Meyer, F. (1994). Topographic distance and watershed lines. *Signal processing, 38*(1), 113-125.

Øren, P. E., & Bakke, S. . (2003). Reconstruction of Berea sandstone and pore-scale modelling of wettability effects. *Journal of Petroleum Science and Engineering, 39(3)*, 177-199.

Rezanezhad, F., Quinton, W. L., Price, J. S., Elrick, D., Elliot, T., & Heck, R. J. (2009). Examining the Effect of Pore Size Distribution and Shape on Flow through Unsaturated Peat using Computer Tomography.

Rosenfeld, A., & Pfaltz, J. L. (1966). Sequential operations in digital picture processing. *Journal of the ACM (JACM), 13*(4), 471-494.

Sheppard, A., Sok, R., & Averdunk, H. (2005). *Improved pore network extraction methods.* Paper presented at the International Symposium of the Society of Core Analysts.

Sheppard, A. P., Sok, R. M., & Averdunk, H. (2004). Techniques for image enhancement and segmentation of tomographic images of porous materials. *Physica A: Statistical Mechanics and its Applications, 339(1)*, 145-151.

Silin, D., & Patzek, T. (2006). Pore space morphology analysis using maximal inscribed spheres. *Physica A: Statistical Mechanics and its Applications, 371*(2), 336-360.

Sime, L., & Ferguson, R. (2003). Information on grain sizes in gravel-bed rivers by automated image analysis. *Journal of Sedimentary Research, 73*(4), 630-636.

Sweeney, S., & Martin, C. (2003). Pore size distributions calculated from 3-D images of DEM-simulated powder compacts. *Acta materialia, 51*(12), 3635-3649.

Wildenschild, D., & Sheppard, A. P. (2013). X-ray imaging and analysis techniques for quantifying pore-scale structure and processes in subsurface porous medium systems. *Advances in Water Resources, 51*, 217-246.

Youssef, S., Rosenberg, E., Gland, N., Bekri, S., & Vizika, O. (2007). Quantitative 3D characterisation of the pore space of real rocks: improved µ-CT resolution and pore extraction methodology. *Society of Core Analysts*, 1-13.

Highlights

- Pore volume segmentation done by an automated watershed algorithm
- Comparison between four different distance functions
- Coordination number distribution of network predicted using watershed segmentation and compared with Maximal ball method